0026-895X/07/7103-695–703$20.00
MOLECULAR PHARMACOLOGY
Copyright © 2007 The American Society for Pharmacology and Experimental Therapeutics
Mol Pharmacol 71:695–703, 2007

Vol. 71, No. 3
26559/3180274
Printed in U.S.A.

The Nucleotide Analog Cidofovir Suppresses Basic Fibroblast Growth Factor (FGF2) Expression and Signaling and Induces Apoptosis in FGF2-Overexpressing Endothelial Cells

Sandra Liekens, Sofie Gijsbers, Els Vanstreels, Dirk Daelemans, Erik De Clercq, and Sigrid Hatse

Rega Institute for Medical Research, Leuven, Belgium

Received May 11, 2006; accepted December 6, 2006

ABSTRACT

Cidofovir [(*S*)-1-(3-hydroxy-2-phosphonylmethoxypropyl)cytosine; (*S*)-HPMPC] is an antiviral drug that has been approved for the treatment of cytomegalovirus retinitis in patients with AIDS. Cidofovir also possesses potent activity against human papillomavirus-induced tumors in animal models and patients. We have recently shown that cidofovir inhibits the development of vascular tumors induced by basic fibroblast growth factor (FGF2)-overexpressing endothelial cells (FGF2-T-MAE) in mice. Here, we demonstrate that the inhibitory activity of cidofovir in FGF2-T-MAE cells may result from the specific induction of apoptosis. Cell cycle analysis revealed that cidofovir induces accumulation of cells in the S phase and, upon prolonged treatment, a significant increase in sub-G_1 cells, exhibiting a subdiploid DNA content. Moreover, annexin V binding, an early event in apoptosis induction, was increased in cidofovir-treated FGF2-T-MAE cells. Cidofovir also caused nuclear fragmentation and the activation of caspase-3-like proteases, as evidenced by the cleavage of poly(ADP-ribose)polymerase. In addition, cidofovir treatment of FGF2-T-MAE cells resulted in a pronounced up-regulation of the tumor suppressor protein p53. However, the expression of Bax and Bcl-2 remained unchanged, and cidofovir did not induce the release of cytochrome *c* from the mitochondria. In addition, cidofovir did not suppress the phosphorylation of protein kinase B/Akt, a transmitter of antiapoptotic survival signals, or its downstream regulator Bad, indicating that the Akt pathway is not affected by cidofovir in FGF2-T-MAE cells. However, the compound inhibited the expression of FGF2 and FGF2 signaling through Erk42/44, as shown by Western blot analysis. Our results indicate that cidofovir inhibits the growth of FGF2-T-MAE cells via inhibition of FGF2 expression and signaling and via the induction of apoptosis. These findings suggest that the clinical use of cidofovir might be expanded to tumors that are not induced by oncogenic viruses.

The acyclic nucleoside phosphonate analog cidofovir [(*S*)-1-(3-hydroxy-2-phosphonylmethoxypropyl) cytosine, (*S*)-HPMPC] (Fig. 1a) is a broad-spectrum anti-DNA virus agent that has been approved for the treatment of cytomegalovirus retinitis in patients with AIDS (De Clercq et al., 1986; De Clercq and Holý, 2005). However, cidofovir also proved effective in various other clinical situations, including the treatment of progressive multifocal leukoencephalopathy, recurrent respiratory papillomatosis, pulmonary papillomatosis, anogenital condylomata acuminata, gingival papillomatous lesions, adenovirus-associated hemorrhagic cystitis, and molluscа contagiosa. In addition, cidofovir is active against poxviruses and is currently the only licensed antiviral drug that has been stockpiled for possible use in the prophylactic therapy of smallpox (De Clercq and Holý, 2005). The antiviral effect of cidofovir results from a selective inhibition of the viral DNA polymerase by its diphosphate metabolite. HPMPCpp acts as a competitive inhibitor/alternative substrate with respect to the natural substrate dCTP. HPMPC is also converted to HPMPCp-choline, which has a very long intracellular half-life of > 80 h and may serve as a reservoir from which the active metabolite HPMPCpp can be continu-

This research was supported by grants from the "Belgische Federatie Tegen Kanker, vzw" (to S.L.), "Geconcerteerde Onderzoeksactie-Vlaanderen (GOA-2005/19), "Impulsefinanciering K. U. Leuven" (to D.D.), and the Centers of Excellence of the Katholieke Universiteit Leuven (Kredietnr EF-05/15; to S.L., S.H., E.D.C.). S.L., D.D., and S.H. are Postdoctoral Researchers of the Fonds voor Wetenschappelijk Onderzoek (FWO)-Vlaanderen.

Article, publication date, and citation information can be found at http://molpharm.aspetjournals.org.

doi:10.1124/mol.106.026559.

ABBREVIATIONS: cidofovir, (*S*)-1-(3-hydroxy-2-phosphonylmethoxypropyl) cytosine, [(*S*)-HPMPC]; EBV, Epstein-Barr virus; HPV, human papillomavirus; FGF2, basic fibroblast growth factor; MAE, murine aortic endothelial; PSS, poly(4-styrenesulfonic acid); DMEM, Dulbecco's modified Eagle's medium; FCS, fetal calf serum; PI, propidium iodide; PBS, phosphate-buffered saline; PARP, poly(ADP-ribose) polymerase; JC-1, 5,5′,6,6′-tetrachloro-1,1′,3,3′-tetraethyl-benzimidazolcarbocyanine iodide; MOPS, 3-(*N*-morpholino)propanesulfonic acid; PCR, polymerase chain reaction.

ously generated, thus explaining the potent antiviral activity of cidofovir upon infrequent dosing (Ho et al., 1992).

Cidofovir has also shown marked antitumor activity in several animal models, including Epstein-Barr virus (EBV)-associated nasopharyngeal carcinoma and human papillomavirus (HPV)-induced cervical carcinoma xenografts in athymic-nude mice, polyomavirus-induced hemangiomas in rats, and hemangiosarcoma development in mice (Andrei et al., 1998; Liekens et al., 1998, 2001c; Neyts et al., 1998; Murono et al., 2001). These tumors are all associated with oncogenic viruses, which encode for cell-transforming proteins that interact with products of tumor suppressor genes. Several reports have indicated that the antitumor effect of cidofovir may result from interference with this interaction (Andrei et al., 2000; Abdulkarim et al., 2002, 2003). However, the potent inhibitory activity of cidofovir on the growth of strongly vascularized tumors of endothelial cell origin (i.e., hemangiomas or hemangiosarcomas) led us to assume that the compound might also possess antiangiogenic properties (Liekens et al., 1998, 2001c).

Angiogenesis is a complex multistep process leading to the formation of new capillary blood vessels. During tumor growth, an intratumoral network of blood vessels is generated to provide the growing tumor with oxygen and nutrients. The new capillaries prevent tumors from undergoing apoptosis and facilitate the escape of tumor cells into the circulation and subsequent metastasis to distant organs (Liekens et al., 2001a; Carmeliet, 2003). Blood vessel formation requires an extensive interplay between cellular and soluble factors with either inhibitory or stimulatory function (Liekens et al., 2001a). One of the best characterized angiogenic factors is basic fibroblast growth factor (FGF2), which has been shown to induce endothelial cell proliferation, chemotaxis, and protease production in vitro and angiogenesis in vivo (Presta et al., 2005). FGF2 has also been implicated in the pathology of angiogenic diseases such as Kaposi's sarcoma and hemangiomas and plays a crucial role in the pathogenesis of several human tumors, including gliomas and hepatocellular carcinoma (Takahashi et al., 1990; Kandel et al., 1991; Takahashi et al., 1994; Presta et al., 2005).

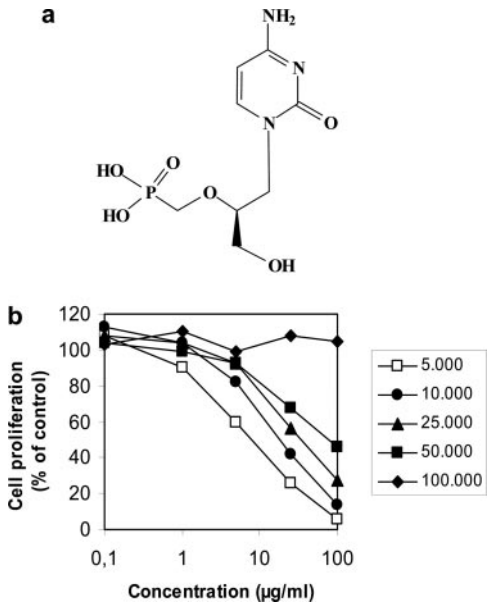

Fig. 1. Chemical structure and antiproliferative activity of cidofovir. a, structure of cidofovir. b, FGF2-T-MAE cells were seeded at 5, 10, 25, 50, or 100 $\times$ 10^3 cells/cm^2 in DMEM with 10% FCS. After 24 h, the medium was replaced, and cidofovir was added. The cell cultures were incubated for 3 days, trypsinized, and counted. The experiments were repeated three times with similar results. Results from one experiment are shown.

Endothelial cells overexpressing FGF2 (FGF2-T-MAE cells) are tumorigenic in athymic-nude mice, giving rise to highly vascularized lesions, which histologically resemble Kaposi's sarcoma (Gualandris et al., 1996; Sola et al., 1997). We have recently shown that intratumoral or systemic cidofovir administration significantly inhibits the growth of subcutaneous, intraperitoneal, and intracerebral FGF2-T-MAE xenografts in athymic nude and *SCID* mice (Liekens et al., 2001b). Cidofovir also completely suppressed hemangioma formation on the chick chorioallantoic membrane induced by intra-allantoic injection of FGF2-*T*-MAE cells, without affecting the normal chorioallantoic membrane vessels. In addition, the drug inhibited the proliferation of primary and transformed endothelial cells but did not affect their capacity to form tube-like structures in fibrin gel or matrigel, indicating that the primary action of cidofovir is not angiostatic (Liekens et al., 2001b).

Because FGF2-T-MAE cells are not associated with an oncogenic virus, we wanted to examine how cidofovir exerts its inhibitory effect on these FGF2-overexpressing endothelial cells. Our results indicate that cidofovir may inhibit the growth of FGF2-T-MAE cells via the inhibition of FGF2 expression and signaling and via the induction of apoptosis.

Materials and Methods

Materials. Cidofovir (Vistide; Fig. 1a) was kindly provided by Gilead Sciences (Foster City, CA). Poly(4-styrenesulfonic acid) (PSS) was provided by Dr. P. Mohan (Chicago, IL).

Cell Cultures. FGF2-transfected mouse aortic endothelial (FGF2-T-MAE) cells express high levels of the M_r 18,000, M_r 22,000, and M_r 24,000 isoforms of FGF2 (Gualandris et al., 1996). FGF2-T-MAE cells were grown in Dulbecco's modified Eagle's medium (DMEM; Invitrogen, Carlsbad, CA) supplemented with 10 mM HEPES (Invitrogen), 10% fetal calf serum (FCS; Harlan Sera-Lab Ltd., Loughborough, UK) and 500 μg/ml Geneticin (Invitrogen).

Cell Proliferation Assays. FGF2-T-MAE cells were seeded at various cell densities (see *Results*) in DMEM with 10% FCS. After 24 h, the medium was replaced and compounds (cidofovir or PSS) were added. The cell cultures were incubated for 3 days, trypsinized, and counted by a Coulter counter (Beckman Coulter, Fullerton, CA).

Flow Cytometric Analysis of Cell Cycle and Apoptosis. FGF2-T-MAE cells were seeded at 20 $\times$ 10^3 cells/cm^2 in DMEM with 10% FCS. After 24 h, the cells were exposed to 50 μg/ml cidofovir or various concentrations of PSS (see *Results*). At different time points, the DNA of the cells was stained with propidium iodide (PI) using the CycleTEST PLUS DNA Reagent Kit (BD Biosciences, San Jose, CA). The DNA content of the stained cell cultures was assessed by flow cytometry on a FACSCalibur flow cytometer equipped with CellQuest software (BD Biosciences) within 3 h after staining (Hatse et al., 1999). Cell debris and clumps were excluded from the analysis by appropriate dot plot gating. Percentages of sub-G_1, G_1, S, and G_2/M cells were estimated using appropriate region markers.

To differentiate between normal (living), apoptotic, and necrotic cells, exponentially growing FGF2-T-MAE cells (seeded at 20 $\times$ 10^3 cells/cm^2) were incubated for 1, 2, 3, or 5 days with or without 50 or 100 μg/ml cidofovir. Cells were then simultaneously stained with annexin-V-FITC and PI using the annexin-V-FITC staining kit (Sigma, St. Louis, MO) and analyzed by flow cytometry. Early apoptotic cells are characterized by high annexin binding and low PI

staining, whereas late apoptotic and necrotic cells stain strongly for both annexin and PI.

DNA Fragmentation Assay. FGF2-T-MAE cells were seeded at 20×10^3 cells/cm^2 in DMEM with 10% FCS. After 24 h, the medium was replaced, and 200 μg/ml cidofovir was added. The cell cultures were incubated for 3 days. Next, cells were lysed, high molecular weight DNA was precipitated, and the cleared supernatants were collected. DNA was precipitated overnight at −20°C. DNA pellets were washed with 70% ethanol and treated with RNase A. The samples were heated at 65°C for 10 min, and DNA was electrophoresed in a 2% agarose gel. Induction of apoptosis is associated with the activation of endonuclease, which cleaves DNA at sites located between nucleosomal units generating mono- and oligonucleosomal DNA fragments.

Western Blot Analysis of FGF2-T-MAE Cell Extracts. FGF2-T-MAE cells were seeded at 20×10^3 cells/cm^2 (unless otherwise stated under *Results*) in flasks containing DMEM with 10% FCS. After 24 h, the medium was replaced, and cidofovir was added. The cell cultures were incubated for 3 days, washed with ice-cold phosphate-buffered saline (PBS) and lysed as described previously (Liekens et al., 1999). Lysates were cleared by centrifugation, and the protein concentration was determined. SDS-polyacrylamide gel electrophoresis of the cell lysates was performed as described previously (Liekens et al., 1999). After electrophoresis, proteins were transferred to pretreated Hybond-P polyvinylidene difluoride membranes (GE Healthcare, Little Chalfont, Buckinghamshire, UK). The membranes were incubated for 1 h at room temperature in blocking buffer (5% nonfat dry milk in PBS containing 0.1% Tween 20) and subsequently for 12 h at 4°C in blocking buffer with primary antibodies raised against β -actin (1/5000; Sigma), FGF2 (clone FB-8, 1/5000; Sigma), Erk42/44 (1/1000; Cell Signaling Technology, Danvers, MA), phospho-Erk42/44 (1/2000; Cell Signaling Technology), Akt (1/1000; Cell Signaling Technology), phospho-Akt (Ser473, 1/1000; Cell Signaling Technology), Bcl-2 (1/1000; Cell Signaling Technology), Bax (1/1000; Cell Signaling Technology), p53 (1/2000; Cell Signaling Technology), or phospho-Bad (Ser136, 1/500; Cell Signaling Technology). To detect cleavage of poly(ADP-ribose) polymerase (PARP) by caspase-3, a primary antibody was used that detects both intact PARP (113 kDa) and the 89-kDa fragment (Roche, Mannheim, Germany). After washing, the membranes were incubated with the corresponding horseradish peroxidase-conjugated secondary antibody (anti-mouse, 1/2000; anti-rabbit, 1/4000; Dako North America, Inc., Carpinteria, CA) in blocking buffer for 25′ at room temperature. Next, the membranes were washed extensively. Immunoreactive proteins were detected by chemiluminescence (ECLplus; Bio-Rad Laboratories, Hercules, CA). Samples were collected from at least two independent experiments and run several times. All images were quantified using ChemiDoc XRS (Bio-Rad Laboratories), and statistical significance of the results was determined by means of the unpaired Student's t test. P values < 0.05 were considered significant.

Measurement of Mitochondrial Membrane Potential. FGF2-T-MAE or HeLa cells were seeded at 20×10^3 cells/cm^2 in flasks containing DMEM with 10% FCS. After 24 h, the medium was replaced, and the cells were treated with cidofovir (100 μg/ml) or actinomycin D (10 μM) for the indicated times (see *Results*). Then, the monolayers were trypsinized, and 10^6 cells were stained with the membrane-permeable fluorochrome JC-1 using the flow cytometry mitochondrial membrane potential detection kit (BD Biosciences) according to the manufacturer's instructions. The cells were analyzed on a FACSCalibur flow cytometer equipped with CellQuest software. JC-1 penetrates the plasma membrane of living cells as a monomer, and its uptake into mitochondria is driven by the mitochondrial membrane potential. Inside the mitochondria, JC-1 aggregates are formed, resulting in a spectral shift toward higher levels of red fluorescence (FL2). Thus, decreased JC-1 fluorescence in the FL2 channel of the flow cytometer is indicative of depolarized mitochondrial membrane.

Cytochrome *c* Release. The apoptosis detection kit was purchased from Mitosciences (Eugene, OR). Immunocytochemical staining of the cells was performed according to the manufacturer's instructions. In brief, FGF2-T-MAE cells were seeded at 20×10^3 cells/cm^2 in flasks containing DMEM with 10% FCS. After 24 h, the medium was replaced, and the cells were treated with cidofovir (100 μg/ml), actinomycin D (10 μM), or staurosporine (1 μM) for the indicated time periods (see *Results*). The cells were fixed with 4% (v/v) paraformaldehyde in PBS for 20 min at room temperature and subsequently permeabilized with 0.1% Triton X-100 in PBS for 15 min. After incubation with 10% goat serum in PBS for 1 h, cells were double-labeled with mouse anti-cytochrome c monoclonal antibody and anti-complex Vα monoclonal antibody (diluted in 10% goat serum in PBS). Complex Vα is part of F_1F_0-ATPase, which is present in the inner mitochondrial membrane. The secondary antibodies were Fluorescein isothiocyanate-conjugated goat anti-mouse IgG2a and Texas Red-conjugated goat anti-mouse IgG2b (diluted in 10% goat serum in PBS). The preparations were analyzed on a Leica TCS SP5 confocal microscope. Cells with punctate cytochrome c staining (green) that overlapped with complex Vα staining (red) were considered as cells with mitochondrial cytochrome c staining, whereas cells that release cytochrome c from the mitochondria should have diffuse nuclear and cytosolic cytochrome c staining and punctate mitochondrial complex Vα staining. Colocalization of cytochrome c and complex Vα was evaluated quantitatively using LAS AF version 1.5.0.

$$R_p = \frac{\sum_I SCh1_I \times SCh2_I}{\sqrt{\sum_I (SCh1_I)^2 \times \sum_I (SCh2_I)^2}}$$

The overlap coefficient, R_p, which describes the extent of overlap between image pairs (0 meaning no overlap and 1 meaning 100% overlap) was used to evaluate colocalization. This coefficient is independent of the intensity variation between channels. $SCh1_I$ and $SCh2_I$ represent the signal intensity of pixels in channel 1 and channel 2, respectively.

To prepare subcellular fractions, cells were harvested in isotonic buffer (5 mM MOPS, 250 mM sucrose, 1 mM EDTA, 1 mM dithiothreitol, and 0.1% EtOH, pH 7.4) supplemented with protease inhibitors (1 mM phenylmethylsulfonyl fluoride and 10 μg/ml leupeptin), and homogenized by 37 strokes in a Dounce homogenizer. The homogenates were centrifuged at 750g for 10 min at 4°C to remove unbroken cells and nuclei. The supernatant was then centrifuged at 10,000g for 30 min at 4°C to obtain the heavy membrane pellet enriched with mitochondria. The resulting supernatant was referred to as the cytosolic fraction. Protein concentration of the different fractions was determined, and SDS-polyacrylamide gel electrophoresis and Western blot analysis were performed as described above, using a primary anti-cytochrome c antibody, provided by Cell Signaling Technology.

RNA Isolation. Total cellular RNA (from three independent cell culture experiments) was isolated using the RNeasy minikit (QIAGEN, Venlo, The Netherlands). RNA was reverse-transcribed to cDNA by means of Moloney murine leukemia virus reverse transcriptase (Invitrogen, Paisley, UK) and random primers (Invitrogen) according to the manufacturer's instructions.

Oligonucleotide Primers and TaqMan Probes. The human FGF2 primers and probe were designed and delivered by Applied Biosystems Assays-on-Demand Gene Expression Products; Assay ID, Hs00266645-m1; Foster City, CA). Mouse β-actin primers and probe were designed with Primer Express (Applied Biosystems). A 138-base-pair fragment of β-actin exon was amplified using primers actin-FW (5′-AGAGGGAAATCGTGCGTGAC-3′) and actin-RV (5′-CAATAGTGATGACCTGGCCGT-3′) and detected by a 23-base-pair probe [5′-(carboxy-4,5-dichloro-2,7-dimethoxyfluorescein)CACTGCCGCATCCTCTTCCTC(5-carboxytetramethylrhodamine)-3′].

Real-Time PCR. Quantitative real-time PCR was performed with an ABI Prism 7000 sequence detection system (Applied Biosystems). All samples were analyzed in triplicate reactions in a final volume of 25 μl containing PCR Master Mix (Eurogentec, Seraing, Belgium), different amounts of primers and probes (β-actin, 120 nM primers and 50 nM probe; FGF-2, 360 nM primers and 100 nM probe), and 30 ng of cDNA template. PCR amplification consisted of 40 cycles of denaturation at 95°C for 15 s and annealing/extension at 60°C for 60 s. The results were evaluated by use of SDS software (Applied Biosystems). Relative quantification of gene expression was performed using the standard curve method. For generation of standard curves, plasmids containing the full-length human FGF2 cDNA (i.e., pJC 119-14, obtained from Prof. M. Presta, University of Brescia, Brescia, Italy) or β-actin was used. For each sample, the relative amount of FGF2 mRNA was determined and normalized to β-actin. For statistical analyses, the Student's t test was calculated. Data are given as mean ± S.E. P values < 0.05 were considered significant.

Results

Cidofovir Treatment Suppresses FGF2-T-MAE Cell Growth and Induces Apoptosis in Vitro. The antiviral drug cidofovir (Fig. 1a) inhibited primary tumor growth of FGF2-T-MAE cells in mice (Liekens et al., 2001b). Because these tumors are not associated with a virus, we wanted to examine how cidofovir suppresses the growth of these FGF2-overexpressing endothelial cells.

We evaluated the antiproliferative effect of cidofovir on FGF2-T-MAE cells, seeded at different cell densities. All nontreated cells grew exponentially over a 4-day period and underwent at least two population doublings (data not shown). Cidofovir suppressed the proliferation of FGF2-T-MAE cells in a dose-dependent manner (Fig. 1b). The inhibitory effect of cidofovir was more pronounced with decreasing initial cell density; i.e., the 50% inhibitory concentration (IC_{50}) was 8, 14, 24, or 35 μg/ml when, respectively, 5, 10, 25, or 50 $\times$ 10^3 FGF2-T-MAE cells/cm^2 were seeded. Cidofovir did not inhibit FGF2-T-MAE proliferation ($IC_{50} > 100$ μg/ml) when 10^5 cells/cm^2 were seeded, indicating that the initial cell density is an important determinant for cidofovir activity. Thus, for all subsequent experiments, cells were seeded at low density (20 $\times$ 10^3 cells/cm^2).

Analysis of cell cycle distribution, via DNA staining with PI, showed that cidofovir (at 50 μg/ml) induces accumulation of FGF2-T-MAE cells in the S phase after 48 h and, upon longer treatment, a significant increase in sub-G_1 cells (19% at day 4), exhibiting a subdiploid DNA content (Fig. 2a), characteristic of apoptotic cells. Apoptosis also results in membrane alterations, including the translocation of phosphatidylserine from the cytoplasmic to the extracellular side of the plasma membrane, where it can be detected by annexin V. Thus, normal (living) cells with low annexin binding and low PI staining, early apoptotic cells with high annexin binding and low PI staining, and necrotic cells with high annexin binding and high PI staining can easily be differentiated (Fig. 2b). Fluorescence-activated cell sorting showed 0.25 to 4.4% of apoptotic cells in control FGF2-T-MAE cell cultures. Cidofovir treatment markedly increased the number of apoptotic cells to 8.4% after 3 days (versus 0.9% in control cells) and up to 78% after 5 days of treatment at 50 μg/ml (versus 4.4% in control cells) (Fig. 2b). Treatment of FGF2-T-MAE cells with cidofovir also resulted in the activation of endonuclease, which cleaves DNA at sites located between nucleosomal units generating mono- and oligonucleosomal DNA fragments, which are absent in DNA from nontreated cell cultures (Fig. 3). These analyses clearly suggest that cidofovir induces apoptosis in cultured FGF2-T-MAE cells.

Cidofovir Induces PARP Cleavage and p53 Up-Regulation in FGF2-T-MAE Cells. PARP is a substrate for the protease caspase-3, which is activated during early stages of apoptosis. The antibody used for Western blot analysis recognizes both uncleaved PARP (113 kDa) and the larger cleavage fragment (89 kDa) (Fig. 4a). After 3 days of treatment with cidofovir, at 50 to 200 μg/ml, a dose-dependent decrease in intact PARP and up to 4-fold increase in the cleaved form of PARP was visible, indicating that caspase-3 is involved in apoptosis induction by cidofovir (Fig. 4a). Protein kinase B/Akt is known to play a critical role in controlling the balance between cell survival and apoptosis (Bellacosa et al., 2005). However, cidofovir suppressed neither the phosphorylation of Akt nor its downstream regulator Bad, indicating that the Akt pathway was not affected by cidofovir treatment of FGF2-T-MAE cells (Fig. 4b). In addition, there was no significant change in the expression of Bcl-2 or Bax after 3 days of exposure to 100 μg/ml cidofovir (Fig. 4c). However, cidofovir (100 μg/ml) induced a 3-fold increase in the expression of the tumor suppressor protein p53 ($p < 0.05$; Fig. 4d).

Cidofovir Induces Apoptosis in FGF2-T-MAE Cells Independently of Cytochrome *c* Release. p53 is an im-

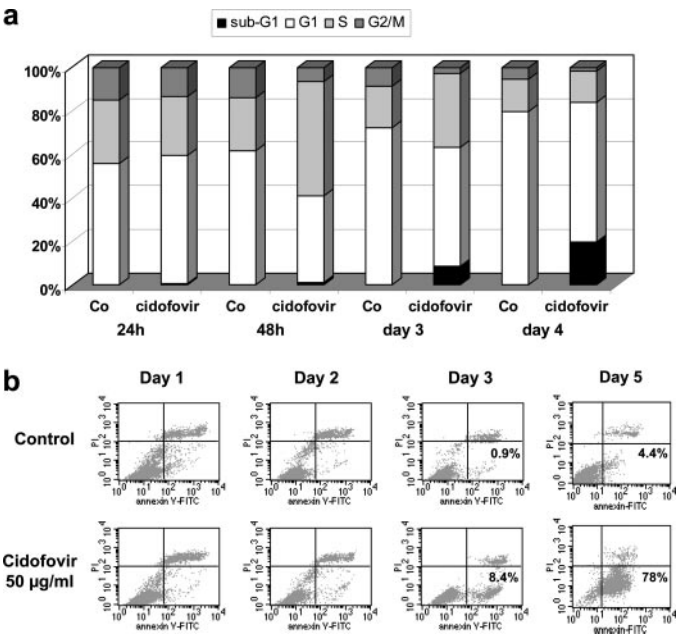

Fig. 2. Flow cytometric analysis of FGF2-T-MAE cells treated with cidofovir. a, exponentially growing FGF2-T-MAE cells were exposed to 50 μg/ml cidofovir. At different time points (i.e., 24, 48, 72, and 96 h), the DNA of the cells was stained with PI and measured by flow cytometry. Cell debris and clumps were excluded from the analysis by appropriate dot plot gating. The percentages of sub-G_1, G_1, S, and G_2/M cells were estimated using appropriate region markers. Co, control. b, FGF2-T-MAE cells were incubated for 1, 2, 3, or 5 days with (bottom row) or without (top row) 50 μg/ml cidofovir. Cells were then stained with annexin-V-FITC and PI and analyzed. Flow cytometric analysis clearly differentiates between normal (living) cells (lower left quadrant) with low annexin and low PI staining, apoptotic cells (lower right quadrant) with high annexin and low PI staining, and necrotic cells (upper right quadrant) with high annexin and high PI staining. The percentages of apoptotic cells at days 3 and 5 are indicated. The experiments were repeated three times with similar results. Results from one experiment are shown.

portant mediator of the mitochondrial pathway of apoptosis, causing cytochrome *c* release and/or depolarization of the mitochondrial membrane (Moll et al., 2005). To evaluate whether cytochrome *c* release is involved in cidofovir-induced apoptosis in FGF2-T-MAE cells, we examined the distribution of cytochrome *c* in subcellular fractions by immunoblotting. The majority of cytochrome *c* remained in the mitochondria-enriched fraction, and there was no detectable increase of cytochrome *c* levels in the cytosolic fractions after cidofovir treatment (100 μg/ml for 2–4 days) of FGF2-T-MAE cells (data not shown). To confirm these findings, we used immunofluorescence microscopy to compare the localization of cytochrome *c* and complex Vα, a mitochondrial protein. Both untreated and cidofovir-treated (100 μg/ml for 2–4 days) FGF2-T-MAE cells showed a mitochondrial distribution of cytochrome *c*, which colocalized with complex Vα (Fig. 5). In addition, treatment with actinomycin D (10 μM, Fig. 5) or staurosporine (1 μM, data not shown), which have been shown to induce cytochrome *c* release in other cell types (Arnoult et al., 2002; Duan et al., 2003), did not cause a diffuse cytosolic staining of cytochrome *c* in FGF2-T-MAE cells, at any of the time points analyzed (8, 10, 12, 14, 18, or 24 h), although cell death was observed.

Moreover, treatment of FGF2-T-MAE cells with cidofovir (100 μg/ml for 2–4 days) did not result in depolarization of the mitochondrial membrane (data not shown). Also actinomycin D (10 μM) did not affect the mitochondrial membrane potential in FGF2-T-MAE cells at any of the time points analyzed (14, 18, or 24 h), whereas depolarization of the mitochondrial membrane was observed in 70% of the actinomycin D-treated HeLa cells after 18 h (data not shown).

Inhibition of FGF2 Expression by Cidofovir in FGF2-T-MAE Cells. Growth factors, including FGF2, can protect cells from undergoing apoptosis. We therefore wanted to investigate whether cidofovir has an effect on FGF2 expression and signaling. FGF2-T-MAE cells express high levels of the M_r 18,000, M_r 22,000, and M_r 24,000 forms of FGF2 (Gualandris et al., 1996) (Fig. 6a). FGF2 expression decreased in a dose-dependent manner after 3 days of treatment with cidofovir [i.e., 38 ± 2% inhibition ($p < 0.05$) at 50 μg/ml to 67 ± 3% inhibition ($p < 0.05$) at 200 μg/ml (Fig. 6a)].

Effect of Cell Density on p53 and FGF2 Expression in FGF2-T-MAE Cells Treated with Cidofovir. Cidofovir inhibited FGF2-T-MAE cell proliferation when ≤50,000 cells/cm^2 were seeded (Fig. 1b). Because the findings described above were obtained with cells, seeded at low density (20×10^3 cells/cm^2), we wanted to know whether the changes in p53 and FGF2 expression, caused by cidofovir, are also influenced by the initial cell number (Fig. 6b). When 10^4/cm^2 FGF2-T-MAE cells were seeded, a 6-fold increase in p53 expression, accompanied by a decrease in FGF2 protein levels of 64 ± 10% ($p < 0.05$), could be noted after 3 days of treatment with 100 μg/ml cidofovir. At higher initial cell densities, the effect of cidofovir was less pronounced (Fig. 6b). In particular, FGF2 levels were unaffected by cidofovir when the initial cell density exceeded 50,000 cells/cm^2 (Fig. 6b). In contrast, cidofovir still induced a 2-fold increase in p53 expression (210 ± 10%, $p < 0.05$) when 10^5 FGF2-T-MAE cells/cm^2 were seeded. Thus, the effects of cidofovir on cell

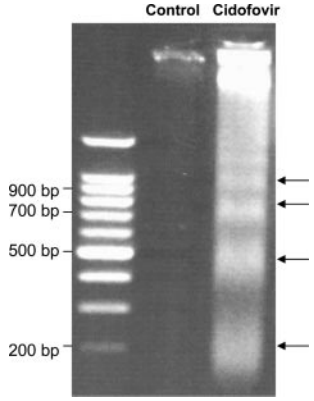

Fig. 3. DNA fragmentation in FGF2-T-MAE cells treated with cidofovir. FGF2-T-MAE cells were seeded at 20×10^3 cells/cm^2 in DMEM with 10% FCS. After 24 h, the medium was replaced, and 200 μg/ml cidofovir was added. The cell cultures were incubated for 3 days. Next, cells were lysed and the isolated DNA was electrophoresed in a 2% agarose gel.

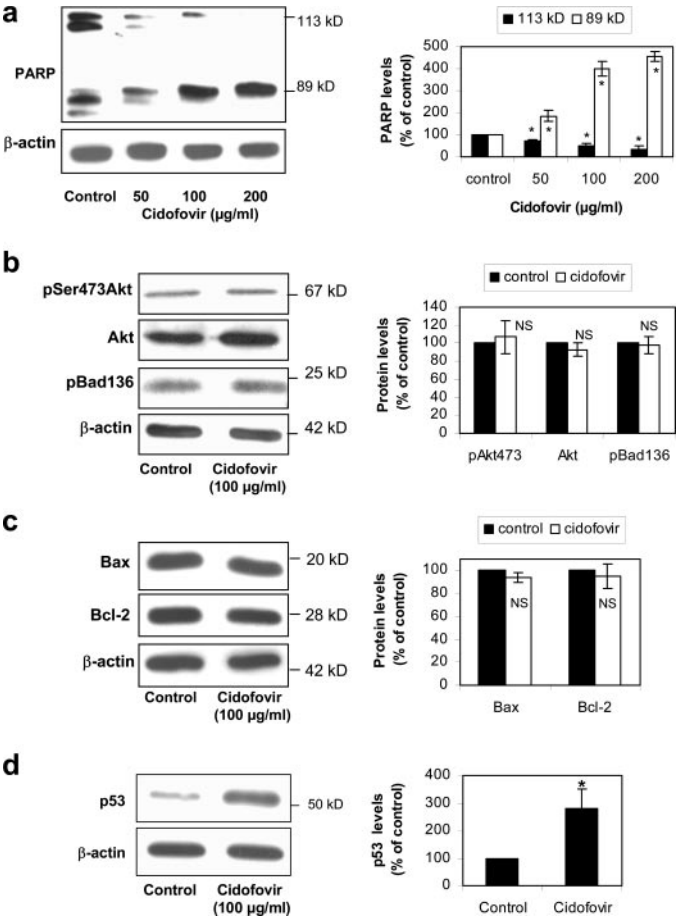

Fig. 4. Biochemical characterization of apoptosis induction in FGF2-T-MAE cells by cidofovir. FGF2-T-MAE cells were seeded at 20×10^3 cells/cm^2 in flasks containing DMEM with 10% FCS. After 24 h, the medium was replaced and cidofovir was added. The cell cultures were incubated for 3 days, washed with PBS, and lysed. Western blot analyses were performed for cleavage of PARP (a), phosphorylation of Akt at Ser473 and Bad at Ser136 (b), Bax and Bcl-2 expression (c), and p53 expression (d). a, bands at 113 and 89 kDa show uncleaved and cleaved forms of PARP, respectively. b, duplicate blots were run simultaneously and probed for total Akt protein. All blots were reprobed for β-actin expression to verify equal protein loading and transfer. Samples were collected from three independent experiments. All images were quantified using ChemiDoc XRS (Bio-Rad Laboratories), and statistical significance of the results was determined by means of the Student's *t* test. Bars represent means (± S.D.). *, $p < 0.05$ (control versus cidofovir-treated cells). NS, not significant.

proliferation, p53, and FGF2 expression are all dependent on the initial FGF2-T-MAE cell density.

In a parallel set of experiments, we quantified FGF2 gene expression levels in untreated and cidofovir-treated FGF2-T-MAE cells by real-time PCR (Fig. 6c). For each sample, the amount of FGF2 mRNA was normalized to β-actin. Statistical analysis was performed on the average values of triplicate reactions from samples taken from three independent experiments. As shown in Fig. 6c, the amount of FGF2 mRNA remained constant as the initial cell density decreased from 10^5 to 2×10^4 cells/cm^2. Only at an initial cell density of 10^4/cm^2 was FGF2 transcription significantly reduced, in both untreated and cidofovir-treated cell cultures ($p < 0.05$). However, cidofovir did not cause a significant down-regulation of FGF2 mRNA expression at any of the cell densities used, indicating that the drug does not inhibit FGF2 transcription.

Inhibition of FGF2 Signaling by Cidofovir in FGF2-T-MAE Cells. Next, we studied the effect of cidofovir on intracellular proteins involved in FGF2 signal transduction. As shown in Fig. 7a, phosphorylation of the mitogen-activated protein kinase Erk42/44 was reduced by 52 ± 22% ($p < 0.05$) in the presence of 100 μg/ml cidofovir, indicating that the drug may inhibit the growth of FGF2-T-MAE cells via inhibition of FGF2 expression and signaling.

We then investigated whether inhibition of FGF2 signaling was sufficient to induce apoptosis in FGF2-T-MAE cells. We showed previously that PSS inhibits FGF2 receptor binding, signaling, and mitogenic activity in endothelial cells at 1 μM (Liekens et al., 1999). Therefore, we treated FGF2-T-MAE cells with increasing concentrations of the FGF2 antagonist. Over a 3-day period, PSS inhibited FGF2-T-MAE cell proliferation with an IC_{50} value of 1.38 ± 18 μM. After 24 h of treatment, PSS (at 0.5 to 2 μM) significantly reduced Erk42/44 phosphorylation, whereas 5 μM PSS was no longer active (Fig. 7b). At 48 and 72 h, PSS inhibited FGF2 signal transduction up to concentrations of 1 μM (not shown). However, the decrease in FGF2 signaling, caused by PSS, was not accompanied by increased p53 expression (Fig. 7b). In fact, PSS treatment even resulted in down-regulation of p53 protein in FGF2-T-MAE cells. To evaluate the effect of PSS on FGF2-T-MAE cell survival, we performed cell cycle analysis of PSS-treated cells (0.5 to 5 μM for 24 to 72 h). PSS (at 5 μM) caused the accumulation of cells in G_1 phase after 48 h (i.e.,

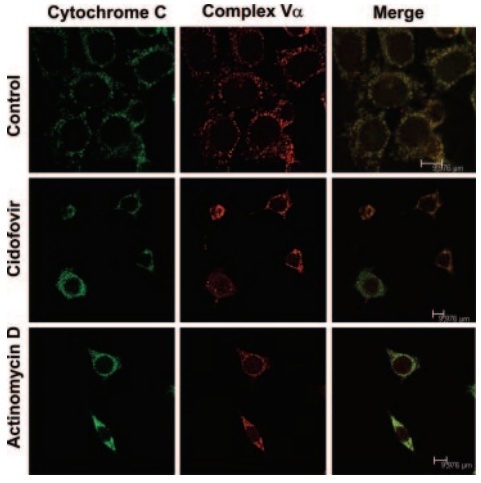

Fig. 5. Distribution of cytochrome *c* in FGF2-T-MAE cells treated with cidofovir. FGF2-T-MAE cells, either untreated (control) or treated with cidofovir (100 μg/ml for 3 days) or actinomycin D (10 μM for 8 h) were fixed and double-labeled with antibodies directed against cytochrome *c* (green) and anti-complex Vα, a protein of the inner mitochondrial membrane (red). The overlap coefficients for control and cidofovir- and actinomycin D-treated cells were 0.82, 0.76, and 0.82, respectively, indicating colocalization of cytochrome *c* with complex Vα.

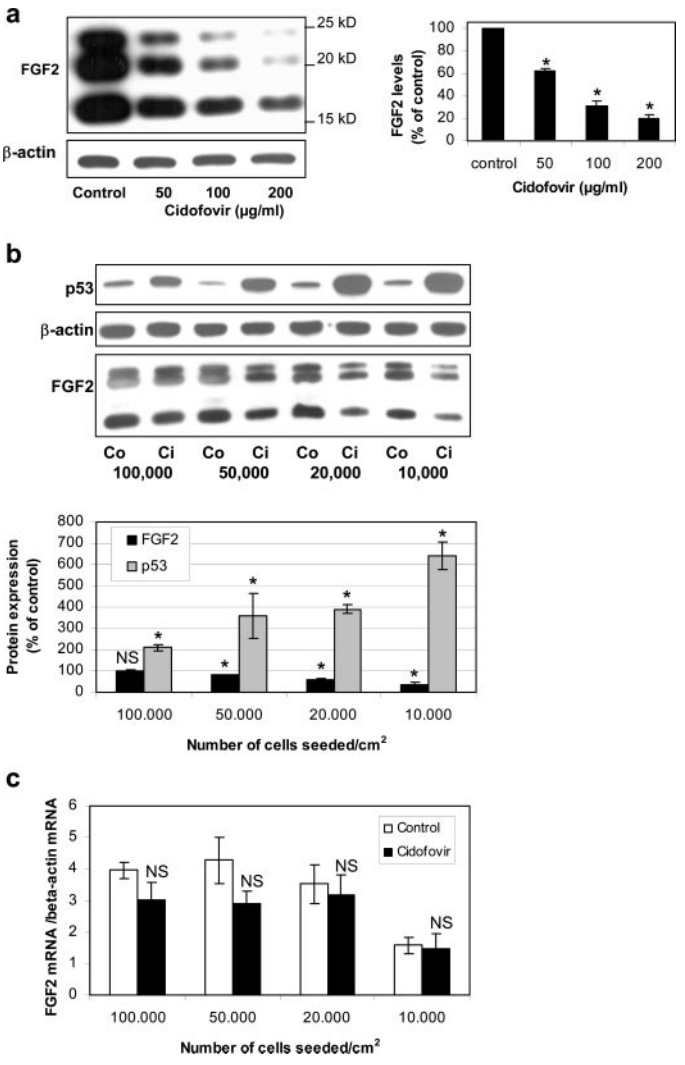

Fig. 6. Effect of cidofovir on FGF2 expression in FGF2-T-MAE cells. a, FGF2-T-MAE cells were seeded at 20×10^3 cells/cm^2 in flasks containing DMEM with 10% FCS. After 24 h, the medium was replaced and cidofovir was added. The cell cultures were incubated for 3 days, cell lysates were collected, and FGF2 expression was determined by Western blot analysis. Samples were collected from three independent experiments. The images were quantified using ChemiDoc XRS (Bio-Rad Laboratories), and statistical significance of the results was determined by means of the Student's *t* test. Bars represent means (± S.D.). *, $p < 0.05$ (control versus cidofovir-treated cells). b, FGF2-T-MAE cells were seeded at 10, 20, 50, or 100×10^3 cells/cm^2 in flasks containing DMEM with 10% FCS. After 24 h, the medium was replaced and 100 μg/ml cidofovir was added. The cell cultures were incubated for 3 days, washed with PBS, and lysed. Western blot analysis was performed for p53 and FGF2 expression. Samples were taken from two independent experiments and run several times. Co, control; Ci, cidofovir. Bars represent expression of p53 and FGF2 in cidofovir-treated cultures, compared with expression of the proteins in control cells with the same seeding density. Bars represent means (± S.E.), *, $p < 0.05$ (control versus cidofovir-treated cells). c, samples collected in b were analyzed in parallel for FGF2 mRNA expression by real-time PCR. For each sample, the relative amount of FGF2 mRNA was determined and normalized to β-actin. For statistical analyses, the unpaired Student's *t* test was calculated. Data are given as means (± S.E.). NS, not significant (control versus cidofovir-treated cells).

MOL PHARM
MOLECULAR PHARMACOLOGY
aspet

81% of PSS-treated cells versus 66% of control cells) (Fig. 7c). However, no apoptotic cells in sub-G_1 phase could be detected at any of the concentrations and time points analyzed. Thus, inhibition of FGF2 signaling is not sufficient for apoptosis induction in FGF2-T-MAE cells.

Discussion

Cidofovir is a potent inhibitor of DNA virus replication, and suppresses the growth of HPV-associated tumors in animal models and patients (De Clercq and Holý, 2005). We have recently shown that cidofovir also inhibits primary FGF2-T-MAE tumor growth in mice (Liekens et al., 2001b). The present study was designed to investigate how cidofovir suppresses the growth of these FGF2-overexpressing endothelial cells that are not associated with an oncogenic virus.

We found that the antiproliferative effect of cidofovir is more pronounced with decreasing initial cell density. When seeded at low density (max. 20×10^3 cells/cm^2), cidofovir induced accumulation of FGF2-T-MAE cells in the S phase and, upon prolonged treatment, a significant increase in sub-G_1 cells. Moreover, cidofovir caused nuclear fragmentation and an increase in annexin V binding, indicating that the cytotoxic activity of cidofovir in FGF2-T-MAE cells is attributed to induction of apoptosis. Thus far, cidofovir has only been shown to cause apoptosis in tumors that are associated with oncogenic viruses, which are known to encode for cell-transforming proteins that interact with products of tumor suppressor genes. Indeed, HPV-associated cancers express E6 and E7 oncoproteins, which bind p53 and retinoblastoma (pRb) tumor suppressor proteins, respectively, and neutralize their function. Cidofovir inhibited E6 and E7 expression, and induced the accumulation of active p53 and pRb in cervical carcinoma. (Abdulkarim et al., 2002). In a number of HPV-positive cell lines, cidofovir was shown to induce apoptosis, which was associated with an increase in p53 and $p21^{WAF\text{-}1}$ (Andrei et al., 2000). Also in patients, cidofovir proved very effective in the treatment of HPV-associated tumors (De Clercq and Holý, 2005). Intratumoral or local administration resulted in complete regression or partial remission of the lesions. Thus, regression of papillomatous tumors upon cidofovir treatment in patients may be due, at least in part, to the induction of apoptosis. Intratumoral or systemic administration of cidofovir has also been shown to inhibit EBV-associated nasopharyngeal carcinoma in mice by induction of apoptosis (Neyts et al., 1998). Also in these experimental models, the apoptotic effect of cidofovir was unrelated to inhibition of the viral DNA polymerase, because the enzyme is not expressed in these latently transfected cells (Murono et al., 2001). In addition, the drug decreased the expression of EBV oncoproteins LMP1 and EBNA2 in EBV-related malignancies, resulting in a decrease of the antiapoptotic Bcl-2 and an increase in the pro-apoptotic Bax protein (Abdulkarim et al., 2003). Based on the above-mentioned findings, it has always been assumed that the antitumor activity of cidofovir results from inhibiting the interactions of viral oncoproteins with products of tumor suppressor genes.

However, FGF2-T-MAE cells are not associated with an oncogenic virus, implying a different mechanism of action of cidofovir in these tumor cells. Indeed, in contrast to EBV-related cancers, the expression of Bcl-2 and Bax remained unchanged after cidofovir treatment of FGF2-T-MAE cells. We next examined the effect of the drug on the serine-threonine kinase Akt/PKB, a transmitter of antiapoptotic survival signals. Activation of the PI3K/Akt pathway has been suggested to be associated with the development of cancer and may allow resistance of cells to a variety of apoptosis-inducing treatments (Bellacosa et al., 2005). Cidofovir did not suppress the phosphorylation of Akt or its downstream regulator Bad, indicating that the Akt pathway is not affected by cidofovir in FGF2-T-MAE cells.

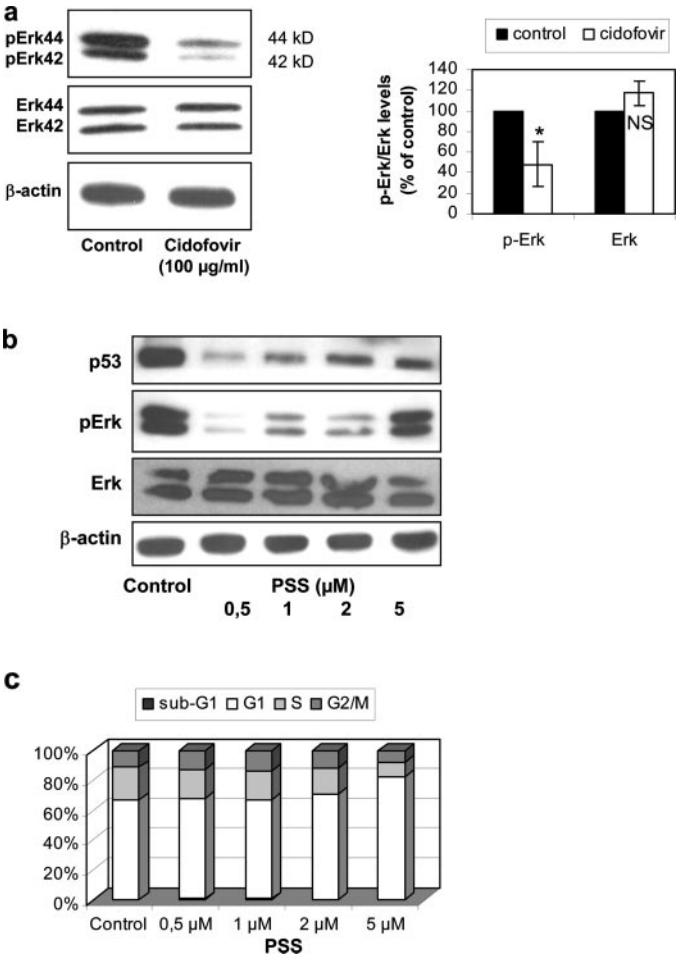

Fig. 7. Inhibition of Erk42/44 phosphorylation is not sufficient for apoptosis induction in FGF2-T-MAE cells. a, FGF2-T-MAE cells were seeded at 20,000 cells/cm^2 in flasks containing DMEM with 10% FCS. After 24 h, the medium was replaced by serum-free DMEM, and cidofovir was added. The cell cultures were incubated for 3 days, washed with PBS, and lysed. Phosphorylation of Erk42/44 was determined by Western blot analysis. Duplicate blots were run simultaneously and probed for total Erk protein. Samples were collected from three independent experiments. The images were quantified using ChemiDoc XRS (Bio-Rad Laboratories), and statistical significance of the results was determined by means of the Student's t test. Bars represent means (± S.D.). *, $p < 0.05$ (control versus cidofovir-treated cells). NS, not significant. b, FGF2-T-MAE cells were seeded at 20×10^3 cells/cm^2 in flasks containing DMEM with 10% FCS. After 24 h, PSS was added. The cell cultures were incubated for another 24 h, washed with PBS, and lysed. Phosphorylation of Erk42/44, total Erk, and p53 expression were determined by Western blot analysis. The experiments were repeated three times with similar results. Results from one experiment are shown. All blots were reprobed for β-actin expression to verify equal protein loading and transfer. c, exponentially growing FGF2-T-MAE cells (see b) were exposed to different concentrations of PSS. After 48 h, the DNA of the cells was stained with PI and measured by flow cytometry. Cell debris and clumps were excluded from the analysis by appropriate dot plot gating. The percentages of sub-G_1, G_1, S, and G_2/M cells were estimated using appropriate region markers.

FGF2-T-MAE cells are murine aortic endothelial cells that overexpress multiple molecular weight isoforms of FGF2 (Gualandris et al., 1996). FGF2 has been shown to stimulate endothelial cell proliferation, migration, and tube formation in vitro and angiogenesis in vivo and can protect cells from undergoing apoptosis (Presta et al., 1986; Gualandris et al., 1996; Liekens et al., 1999; Hotfilder et al., 2005; Presta et al., 2005; Vandermoere et al., 2005). Cidofovir treatment of FGF2-T-MAE cells resulted in a pronounced reduction of FGF2 protein expression and signaling through Erk42/44, as shown by Western blot analysis. However, quantitative RT-PCR did not reveal a significant down-regulation of FGF2 mRNA expression by cidofovir, indicating that the drug does not inhibit FGF2 transcription. Moreover, the FGF2 antagonist PSS, which inhibits Erk42/44 phosphorylation and FGF2-induced proliferation (Liekens et al., 1999), did not cause apoptosis in FGF2-T-MAE cells, indicating that inhibition of FGF2 signaling is not sufficient for apoptosis induction in these cells. In addition, addition of exogenous FGF2 (25–500 ng/ml) could not prevent cidofovir-induced FGF2-T-MAE cell death (data not shown).

Cidofovir caused a significant up-regulation of the tumor suppressor p53. p53 induces either cell cycle arrest by transactivation of p21 or apoptosis through transcription-dependent and -independent mechanisms (Waldman et al., 1995; Polyak et al., 1997; reviewed in Moll et al., 2005 and Resnick-Silverman and Manfredi, 2006). Nuclear p53 may increase the expression of death receptors, pro-apoptotic proteins such as Bax, Bid, Noxa, and PUMA, and redox-related genes (Polyak et al., 1997; Resnick-Silverman and Manfredi, 2006). Cytosolic or mitochondrial p53 may directly activate Bax/Bak via transcription-independent mechanisms, and neutralize the antiapoptotic effect of Bcl-2/Bcl-X_L, resulting in the permeabilization of the mitochondrial outer membrane, the subsequent release of cytochrome *c*, and caspase-3 activation (Mihara et al., 2003; Chipuk et al., 2004; Leu et al., 2004). We did not observe changes in the expression of Bax or Bcl-2 after cidofovir treatment of FGF2-T-MAE cells. In addition, cidofovir did not cause the release of cytochrome *c* from the mitochondria. In addition, actinomycin D and staurosporine, which have been shown to induce cytochrome *c* release in various cell types (Arnoult et al., 2002; Duan et al., 2003), caused the death of FGF2-T-MAE cells without affecting cytochrome *c* localization. Previous reports indicate that p53 may also induce cytochrome *c*-independent apoptosis in certain cell types (Li et al., 1999). In HeLa cells that were transduced to overexpress p53, apoptosis was induced by reactive oxygen species-mediated disruption of the mitochondrial membrane potential, in the absence of cytochrome *c* release (Li et al., 1999). However, cidofovir did not affect the mitochondrial membrane potential in FGF2-T-MAE cells (not shown). In addition, actinomycin D, which strongly induced depolarization of the mitochondrial membrane in HeLa cells, had no effect on the mitochondrial potential in FGF2-T-MAE cells (data not shown). These findings indicate that apoptosis induction in FGF2-T-MAE cells may occur without involvement of the mitochondria. However, we did observe the cleavage of the caspase-3 substrate poly(ADP-ribose)polymerase, suggesting that apoptosis stimulation by cidofovir in FGF2-T-MAE cells is caspase-dependent.

Recent studies using knockout mouse models have provided evidence for the existence of several novel p53 targets, including *Noxa*, *Puma,* and *Perp* (Ihrie et al., 2003; Jeffers et al., 2003; Shibue et al., 2003; Villunger et al., 2003). These studies have shown that the role of each target gene is dependent on the cell type and apoptotic stimulus. Noxa and Puma are members of the Bcl-2 family of apoptotic regulators, which act on mitochondria to stimulate apoptosis (Villunger et al., 2003). In contrast, Perp represents a novel type of p53 effector that localizes to the plasma membrane rather than to the mitochondria (Attardi et al., 2000; Ihrie et al., 2003). Thus, the up-regulation of p53 upon cidofovir treatment of FGF2-T-MAE cells may lead to apoptosis via alternative routes yet to be identified. It should be noted that cidofovir has been shown to possess potent antitumor activity against EBV-associated nasopharyngeal carcinoma in mice with xenografts that contain mutant p53 genes, indicating that cidofovir may also induce p53-independent apoptosis (Neyts et al., 1998). In fact, several reports indicate that, in certain cell types, DNA damaging agents may induce apoptosis via Fas signaling, leading to caspase-8 activation and the direct activation of caspase-3 in the absence of mitochondrial involvement (Kasibhatla et al., 1998, Huang et al., 2003).

p53 also participates in post-transcriptional control processes. In human skin fibroblasts, an inverse correlation was shown between p53 expression and FGF2 mRNA translation efficiency (Galy et al., 2001a,b). Thus, increased expression of p53 protein by cidofovir may cause a reduction in FGF2 levels by a post-transcriptional mechanism, resulting in the inhibition of FGF2 signal transduction and reduced proliferative capacity of FGF2-T-MAE cells. Our results suggest that cidofovir affects FGF2 translation and/or degradation. Because increased p53 expression is accompanied by reduced FGF2 levels in cidofovir-treated FGF2-T-MAE cells, p53 may contribute to the reduction in FGF2 levels. However, upon seeding of FGF2-T-MAE cells at high cell density (i.e., 10^5 cells/cm^2) cidofovir induced a 2-fold increase in p53 expression, whereas FGF2 mRNA and protein remained constant. Thus, under these conditions, increased expression of p53 was not sufficient to cause a decrease in FGF2 protein levels.

Taken together, our data indicate that cidofovir increased p53 expression and caused caspase-dependent apoptosis in FGF2-T-MAE cells, although the molecular mechanisms linking p53 to caspase-3 remain unclear. The marked antitumor effect of cidofovir in mice inoculated with FGF2-T-MAE cells is probably due to the induction of apoptosis. Cidofovir may thus also be useful in a clinical setting to prevent the progression of tumors that are not associated with an oncogenic virus, which would considerably expand the antitumor spectrum of cidofovir.

Acknowledgments

We are grateful to Prof. Marco Presta (Brescia, Italy) and Prof. Jan Balzarini (Leuven, Belgium) for suggestions and critical reading of the manuscript.

References

Abdulkarim B, Sabri S, Deutsch E, Chagraoui H, Maggiorella L, Thierry J, Eschwege F, Vainchenker W, Chouaib S, and Bourhis J (2002) Antiviral agent Cidofovir restores p53 function and enhances the radiosensitivity in HPV-associated cancers. *Oncogene* **21:**2334–2346.

Abdulkarim B, Sabri S, Zelenika D, Deutsch E, Frascogna V, Klijanienko J, Vainchenker W, Joab I, and Bourhis J (2003) Antiviral agent cidofovir decreases Epstein-Barr virus (EBV) oncoproteins and enhances the radiosensitivity in EBV-related malignancies. *Oncogene* **22:**2260–2271.

Andrei G, Snoeck R, Piette J, Delvenne P, and De Clercq E (1998) Inhibiting effects

of cidofovir (HPMPC) on the growth of the human cervical carcinoma (SiHa) xenografts in athymic nude mice. *Oncol Res* **10:**533–539.
Andrei G, Snoeck R, Schols D, and De Clercq E (2000) Induction of apoptosis by cidofovir in human papillomavirus (HPV)-positive cells. *Oncol Res* **12:**397–408.
Arnoult D, Parone P, Martinou J-C, Antonsson B, Estaquier J, and Ameisen JC (2002) Mitochondrial release of apoptosis-inducing factor occurs downstream of cytochrome *c* release in response to several proapoptotic stimuli. *J Cell Biol* **159:**923–929.
Attardi LD, Reczek EE, Cosmas C, Demicco EG, McCurrach ME, Lowe SW, and Jacks T (2000) Perp, an apoptosis-associated target of p53, is a novel member of the PMP-22/gas3 family. *Genes Dev* **14:**704–718.
Bellacosa A, Kumar CC, Di Cristofano A, and Testa JR (2005) Activation of AKT kinases in cancer: implications for therapeutic targeting. *Adv Cancer Res* **94:**29–86.
Carmeliet P (2003) Angiogenesis in health and disease. *Nat Med* **9:**653–660.
Chipuk JE, Kuwana T, Bouchier-Hayes L, Droin NM, Newmeyer DD, Schuler M, and Green DR (2004) Direct activation of Bax by p53 mediates mitochondrial membrane permeabilization and apoptosis. *Science (Wash DC)* **303:**1010–1014.
De Clercq E, Holý A, Rosenberg I, Sakuma T, Balzarini J, and Maudgal PC (1986) A novel selective broad-spectrum anti-DNA virus agent. *Nature (Lond)* **323:**464–467.
De Clercq E and Holý A (2005) Acyclic nucleoside phosphonates: a key class of antiviral drugs. *Nat Rev Drug Discov* **4:**928–940.
Duan S, Hájek P, Lin C, Shin SK, Attardi G, and Chomyn A (2003) Mitochondrial outer membrane permeability change and hypersensitivity to digitonin early in staurosporine-induced apoptosis. *J Biol Chem* **278:**1346–1353.
Galy B, Creancier L, Prado-Lourenco L, Prats AC, and Prats H (2001a) p53 directs conformational change and translation initiation blockade of human fibroblast growth factor 2 mRNA. *Oncogene* **20:**4613–4620.
Galy B, Creancier L, Zanibellato C, Prats AC, and Prats H (2001b) Tumour suppressor p53 inhibits human fibroblast growth factor 2 expression by a post-transcriptional mechanism. *Oncogene* **20:**1669–1677.
Gualandris A, Rusnati M, Belleri M Nelli EE, Bastaki M, Molinari-Tosatti MP, Bonardi F, Parolini S, Albini A, Morbidelli L, Ziche M, et al. (1996) Basic fibroblast growth factor overexpression in endothelial cells: an autocrine mechanism for angiogenesis and angioproliferative diseases. *Cell Growth Differ* **7:**147–160.
Hatse S, Schols D, De Clercq E, and Balzarini J (1999) 9-(2Phosphonylmethoxyethyl) adenine induces tumor cell differentiation or cell death by blocking cell cycle progression through the S phase. *Cell Growth Differ* **10:**435–446.
Ho HT, Woods KL, Bronson JJ, De Boeck H, Martin JC, and Hitchcock MJ (1992) Intracellular metabolism of the antiherpes agent (*S*)-1-[3-hydroxy-2-(phosphonylmethoxy)propyl]cytosine. *Mol Pharmacol* **41:**197–202.
Hotfilder M, Sondermann P, Senss A, van Valen F, Jurgens H, and Vormoor J (2005) PI3K/AKT is involved in mediating survival signals that rescue Ewing tumour cells from fibroblast growth factor 2-induced cell death. *Br J Cancer* **92:**705–710.
Huang HL, Fang LW, Lu SP, Chou CK, Luh TY, and Lai MZ (2003) DNA-damaging reagents induce apoptosis through reactive oxygen species-dependent Fas aggregation. *Oncogene* **22:**8168–8177.
Ihrie RA, Reczek E, Horner JS, Khachatrian L, Sage J, Jacks T, and Attardi LD (2003) Perp is a mediator of p53-dependent apoptosis in diverse cell types. *Curr Biol* **13:**1985–1990.
Jeffers JR, Parganas E, Lee Y, Yang C, Wang J, Brennan J, MacLean KH, Han J, Chittenden T, Ihle JN, et al. (2003) Puma is an essential mediator of p53-dependent and -independent apoptotic pathways. *Cancer Cell* **4:**321–328.
Kandel J, Bossy-Wetzel E, Radvanyi F, Klagsbrun M, Folkman J, and Hanahan D (1991) Neovascularization is associated with a switch to the export of bFGF in the multistep development of fibrosarcoma. *Cell* **66:**1095–1104.
Kasibhatla S, Brunner T, Genestier L, Echeverri F, Mahboubi A, and Green DR (1998) DNA damaging agents induce expression of Fas ligand and subsequent apoptosis in T lymphocytes via the activation of NF-kappa B and AP-1. *Mol Cell* **1:**543–551.
Leu JI, Dumont P, Hafey M, Murphy ME, and George DL (2004) Mitochondrial p53 activates Bak and causes disruption of a Bak-Mcl1 complex. *Nat Cell Biol* **6:**443–450.
Li P-F, Dietz R, and von Harsdorf R (1999) p53 regulates mitochondrial membrane potential through reactive oxygen species and induces cytochrome *c*-independent apoptosis blocked by Bcl-2. *EMBO (Eur Mol Biol Organ) J* **18:**6027–6036.
Liekens S, Andrei G, Vandeputte M, De Clercq E, and Neyts J (1998) Potent inhibition of hemangioma formation in rats by the acyclic nucleoside phosphonate analogue cidofovir. *Cancer Res* **58:**2562–2567.
Liekens S, De Clercq E, and Neyts J (2001a) Angiogenesis: regulators and clinical applications. *Biochem Pharmacol* **61:**253–270.
Liekens S, Leali D, Neyts J Esnouf R, Rusnati M, Dell'Era P, Maudgal PC, De Clercq E, and Presta M (1999) Modulation of fibroblast growth factor-2 receptor binding, signaling, and mitogenic activity by heparin-mimicking polysulfonated compounds. *Mol Pharmacol* **56:**204–213.
Liekens S, Neyts J, De Clercq E, Verbeken E, Ribatti D, and Presta M (2001b) Inhibition of fibroblast growth factor-2-induced vascular tumor formation by the acyclic nucleoside phosphonate cidofovir. *Cancer Res* **61:**5057–5064.
Liekens S, Verbeken E, De Clercq E, and Neyts J (2001c) Potent inhibition of hemangiosarcoma development in mice by cidofovir. *Int J Cancer* **92:**161–167.
Mihara M, Erster S, Zaika A, Petrenko O, Chittenden T, Pancoska P, and Moll UM (2003) p53 has a direct apoptogenic role at the mitochondria. *Mol Cell* **11:**577–590.
Moll UM, Wolff S, Speidel D, and Deppert W (2005) Transcription-independent pro-apoptotic functions of p53. *Curr Opin Cell Biol* **17:**631–636.
Murono S, Raab-Traub N, and Pagano JS (2001) Prevention and inhibition of nasopharyngeal carcinoma growth by antiviral phosphonated nucleoside analogs. *Cancer Res* **61:**7875–7877.
Neyts J, Sadler R, De Clercq E, Raab-Traub N, and Pagano JS (1998) The antiviral agent cidofovir[(*S*)-1-(3-hydroxy-2-phosphonyl-methoxypropyl)cytosine] has pronounced activity against nasopharyngeal carcinoma grown in nude mice. *Cancer Res* **58:**384–388.
Polyak K, Xia Y, Zweier JL, Kinzler KW, and Vogelstein B (1997) A model for p53-induced apoptosis. *Nature (Lond)* **389:**300–305.
Presta M, Moscatelli D, Joseph-Silverstein J, and Rifkin DB (1986) Purification from a human hepatoma cell line of a basic fibroblast growth factor-like molecule that stimulates capillary endothelial cell plasminogen activator production, DNA synthesis, and migration. *Mol Cell Biol* **6:**4060–4066.
Presta M, Dell'Era P, Mitola S, Moroni E, Ronca R, and Rusnati M (2005) Fibroblast growth factor/fibroblast growth factor receptor system in angiogenesis. *Cytokine Growth Factor Rev* **16:**159–178.
Resnick-Silverman L and Manfredi JJ (2006) Gene-specific mechanisms of p53 transcriptional control and prospects for cancer therapy. *J Cell Biochem* **99:**679–689.
Shibue T, Takeda K, Oda E, Tanaka H, Murasawa H, Takaoka A, Morishita Y, Akira S, Taniguchi T, and Tanaka N (2003) Integral role of Noxa in p53-mediated apoptotic response *Genes Dev* **17:**2233–2238.
Sola F, Gualandris A, Belleri M, Giuliani R, Coltrini D, Bastaki M, Tosatti MP, Bonardi F, Vecchi A, Fioretti F, et al. (1997) Endothelial cells overexpressing basic fibroblast growth factor (FGF-2) induce vascular tumors in immunodeficient mice. *Angiogenesis* **1:**102–106.
Takahashi JA, Mori H, Fukumoto M, Igarashi K, Jaye M, Oda Y, Kikuchi H, and Hatanaka M (1990) Gene expression of fibroblast growth factors in human gliomas and meningiomas: demonstration of cellular source of basic fibroblast growth factor mRNA and peptide in tumor tissues. *Proc Natl Acad Sci USA* **87:**5710–5714.
Takahashi K, Mulliken JB, Kozakewich HP, Rogers RA, Folkman J, and Ezekowitz RA (1994) Cellular markers that distinguish the phases of hemangioma during infancy and childhood. *J Clin Investig* **93:**2357–2364.
Vandermoere F, El Yazidi-Belkoura I, Adriaenssens E, Lemoine J, and Hondermarck H (2005) The antiapoptotic effect of fibroblast growth factor-2 is mediated through nuclear factor-kappaB activation induced via interaction between Akt and IkappaB kinase-beta in breast cancer cells. *Oncogene* **24:**5482–5491.
Villunger A, Michalak EM, Coultas L, Mullauer F, Bock G, Ausserlechner MJ, Adams JM, and Strasser A (2003) p53- and drug-induced apoptotic responses mediated by BH3-only proteins puma and noxa. *Science (Wash DC)* **302:**1036–1038.
Waldman T, Kinzler KW, and Vogelstein B (1995) p21 is necessary for the p53-mediated G_1 arrest in human cancer cells. *Cancer Res* **55:**5187–5190.

Address correspondence to: Dr. Sandra Liekens, Laboratory of Virology and Chemotherapy, Rega Institute for Medical Research, Minderbroedersstraat 10, B-3000 Leuven, Belgium. E-mail: sandra.liekens@rega.kuleuven.be